

# Design of a Solar Motor Drive System Fed by a Direct-Connected Photovoltaic Array

Omur AYDOGMUS

Department of Electrical and Electronics Eng., Faculty of Technology, Firat University, 23119, Turkey  
oaydogmus@firat.edu.tr

**Abstract**—A solar motor pump drive system is modeled and simulated. The proposed drive system does not require any kind of energy storage system and dc-dc converter. The system is connected directly to a photovoltaic (PV) array. Thus, a low cost solar system can be achieved. A vector controlled Permanent Magnet Synchronous Motor (PMSM) is used as a solar motor to increase the efficiency of system. The motor is designed for a low rated voltage level about 24V. The hill climbing MPPT method is used for balanced the motor power and PV power to obtain a high efficiency. The results are performed by using MATLAB/SimPowerSystem blocks. In addition, the PV array is modeled to allow for the possibility of running as on-line adjustable in simulation environment without using lookup table. The performances of motor, MPPT and drive system are analyzed in different conditions as temperature and irradiation of PV array.

**Index Terms**—maximum-power-point-tracking method, permanent magnet motor, photovoltaic systems, solar power generation, space vector PWM.

## I. INTRODUCTION

The electric energy consumption is one of the most essential part of life which is continuously increasing [1]. The increasing of consumption cannot be stopped completely, so the generation of electrical energy is increased depend on value of consumption. As another solution, the total consumption can be reduced by increasing the efficiency of systems. Furthermore, the renewable energy should be used to meet demand of electric energy [2].

Today, the popularity of solar and wind power generation rapidly increases since they have had a high potential resource. For instance, according to the U.S. Department of Energy, the solar energy resource from a 100-mile-square area of Nevada could supply the U.S. with all its electricity about 800 GW, using modestly efficient %10 commercial PV modules [3]. As a huge alternative, the potential of solar power energy can be used instead of fossil fuels and uranium [4–7]. According to IMS research, global solar PV installations are reached up to about 20 GW in 2011 [8–9].

The commercial PV modules have not sufficient capacity for obtaining a high ratio of power/area (W/m<sup>2</sup>). Therefore, the efficiency of PVs should be significantly increased to improve solar power generation system [10]. This is not enough to improve the total efficiency of solar power system. In addition, all parts of the solar power system such as a dc/ac inverter and load should be had a high efficiency to obtain an effective system.

The dc/ac conversion is widely performed by using

voltage source inverters in PV systems. In these systems, the dc-link voltage of the inverter should be controlled since the output voltage of the PV modules varies with temperature, irradiance, and the effect of MPPT [11]. The MPPT method is usually an essential part of a PV power generation system, because of the nonlinear characteristics of the PV array [12]. Generally, the PV systems require batteries, charger, boost converter and inverter as shown in Fig.1. In this connection, the MPPT is obtained by controlling the battery charger or boost converter to improve the efficiency of the system. It can be seen that the system cost is increased due to the usage of such a connection.

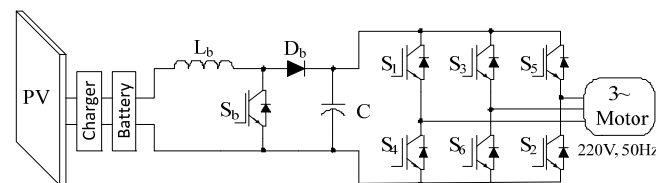


Figure 1. Traditional installation of the solar system

A motor can be designed for a low rated voltage level as an alternative for the traditional installation of solar system. Thus, the PV voltage can be directly used without using a boost converter. Besides, the MPPT can be achieved by controlling the motor current and speed. This simple connection has some advantages such as not required boost converter, battery and its charger. As a disadvantage, it can be said that this system can only worked in daylight. If there is a requirement for working during the whole day, a storage system can be easily added to this system.

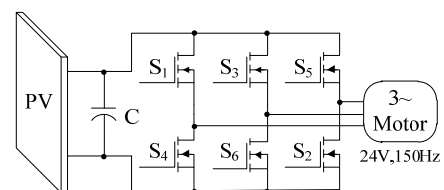


Figure 2. Proposed installation of the solar system

The electric motors play an essential role in these systems since the system efficiency is directly affected from the efficiency of motor and its drive. Electrical motor drive systems are used to control the machine parameters such as direction, speed and torque during transient and steady-state conditions. The asynchronous machines with cage rotor type are preferred to the other type of machines in many applications because of their robust structures and low cost. However, they have not a high efficiency more than the PMSMs which have a high performance, good dynamic response, high torque, low inertia, high efficiency, high

power density, durability and reliability. In addition, the permanent magnet rotor has many advantages including the elimination of brushes slip-rings and rotor chopper losses in the field winding which leads to higher efficiency. The higher efficiency allows a reduction in the machine frame size [12-16].

In this paper, a drive system is performed for a PMSM which is fed by a direct-connected PV array. The motor, PWM algorithm, drive system, PV model and MPPT are given in details. The PV array is modeled to allow for the possibility of running as on-line adjustable in simulation environment without using lookup table. The performances of motor, MPPT and drive system are analyzed in different conditions as temperature and irradiation of PV array. The results are obtained by using MATLAB/SimPowerSystem blocks.

## II. CONTROL DESIGN OF THE SOLAR MOTOR

The electric motors should be controlled to improve the efficiency of system especially which are fed by a solar energy power source. The squirrel cage induction motors are widely used in these applications which require boosted voltage to obtain rated voltage [17]. For instance, a three-phase induction motor (220Vac, 50 Hz and 2 poles) requires a boosted voltage which is stepped up from 12-24Vdc up to 300Vdc for working in a solar power system. In contrast, the motor can be designed with a low voltage as 24V which is not required a boosted voltage. Thus, the motor drive system can be directly connected to the solar PV panels. For this purpose, a PMSM is used to obtain high efficiency at low voltage.

The voltage equations of PMSM are given as;

$$u_d(t) = R_s i_d(t) + \frac{d\psi_d(t)}{dt} - \omega_e \psi_q(t) \quad (1)$$

$$u_q(t) = R_s i_q(t) + \frac{d\psi_q(t)}{dt} + \omega_e \psi_d(t) \quad (2)$$

where  $\omega_e$  is the electrical rotor frequency,  $R_s$  is the stator winding resistance.  $\psi_d$  and  $\psi_q$  are linkage fluxes of d-axis and q-axis, respectively. The linkage fluxes are given in Eq.3 and Eq.4

$$\psi_d = L_d i_d + \psi_m \quad (3)$$

$$\psi_q = L_q i_q \quad (4)$$

where  $\psi_m$  is the flux linkage due to the rotor magnets. The electromagnetic torque for synchronous machines in the d, q-axis is given by:

$$T_e = \frac{3}{2} p [\psi_d i_q - \psi_q i_d] \quad (5)$$

where  $p$  is pole pairs number. If Eq. 3 and Eq. 4 are substituted into Eq. 5, the torque can also be expressed in the following way.

$$T_e = \frac{3}{2} p [\psi_m i_q + (L_d - L_q) i_d i_q] \quad (6)$$

The mechanical equation is given by;

$$T_e = T_L + J \frac{d\omega_m}{dt} + B \omega_m \quad (7)$$

where  $J$  is inertia,  $B$  is the friction coefficient,  $T_L$  is load torque and  $\omega_m$  is mechanical angular velocity of the rotor which is defined as  $\omega_e = p \omega_m$ . The controllers are designed by using internal model control method. Details of the speed and current controllers' design can be found in [18, 19]. The vector control diagram of the PMSM is shown in Fig.3 obtained by using MATLAB.

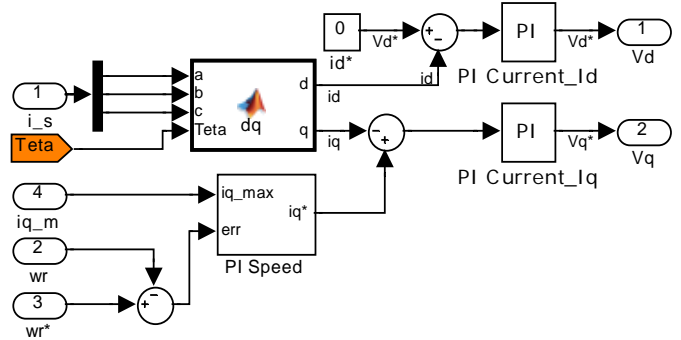


Figure 3. Vector control blocks

The parameters of current controllers can be determined with Eq.8 and Eq.9.

$$k_{pd} = \alpha_c L_d, \quad k_{id} = \alpha_c (R_s + R_{ad}), \quad R_{ad} = \alpha_c L_d - R_s \quad (8)$$

$$k_{pq} = \alpha_c L_q, \quad k_{iq} = \alpha_c (R_s + R_{aq}), \quad R_{aq} = \alpha_c L_q - R_s \quad (9)$$

where  $\alpha_c$  is design parameters which is determined by desired rise time. Thus, the current controllers are expressed by using only motor parameters and rise time without using root locus analysis and Bode plots [18]. The parameters of speed controller are given in Eq.10.

$$k_{ps} = \frac{J \alpha_s}{p K_t}, \quad k_{is} = \frac{J \alpha_s^2}{p K_t} \quad (10)$$

where  $\alpha_s$  is the bandwidth of the speed controller.  $\alpha_s$  depends on the desired rise time of the speed loop  $K_t$  is torque constant of motor.

The  $V_d$  and  $V_q$  voltages calculated by vector control algorithm to apply PWM algorithm.

## III. SPACE VECTOR PWM TECHNIQUE

The space vector PWM (SVPWM) is widely used for controlling inverter since it can be allowed an easy implementation.  $V_\alpha$  and  $V_\beta$  should be used to determine the reference vector expressed in Eq.11, Eq.12 and Eq.13.

$$V_\alpha = V_d \cos(\theta) - V_q \sin(\theta) \quad (11)$$

$$V_\beta = V_d \sin(\theta) + V_q \cos(\theta) \quad (12)$$

where  $V_d$  and  $V_q$  are given from outputs of vector control algorithm.  $\theta$  is angle of the reference vector depend on the rotor position. The reference vector is determined as;

The switches are connected to positive and negative side of inverter combined as 111 and 000, respectively. The combination of 000 is not used for five-segment switching sequence [20]. Thus, the switching losses are reduced by using the five-segment switching sequence shown in Fig.4. The possible vectors ( $V_1$  to  $V_7$ ) and switching sequences of each sector are given in Fig.4.

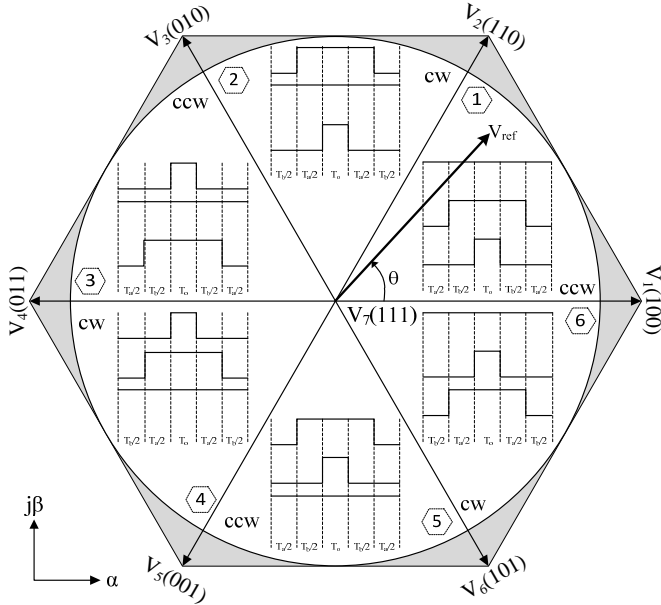


Figure 4. Switching sequences with space vectors

The dwell times are calculated depending on sector, modulation index and angle of vector. The modulation index is expressed as shown in Eq.14.

$$m = \sqrt{V_\alpha^2 + V_\beta^2} \text{ or } m = \frac{V_{ref} \sqrt{3}}{V_{dc}} \quad (14)$$

The calculation of the dwell times are given in Eq.15 to Eq.18.

TABLE I. TIMING CALCULATIONS

Sector	Switch	Switching Times
1	S1	$TU = Ta + Tb + To$
	S2	$TV = Tb + To$
	S3	$TW = To$
2	S1	$TU = Ta + To$
	S2	$TV = Ta + Tb + To$
	S3	$TW = To$
3	S1	$TU = To$
	S2	$TV = Ta + Tb + To$
	S3	$TW = Tb + To$
4	S1	$TU = To$
	S2	$TV = Ta + To$
	S3	$TW = Ta + Tb + To$
5	S1	$TU = Tb + To$
	S2	$TV = To$
	S3	$TW = Ta + Tb + To$
6	S1	$TU = Ta + Tb + To$
	S2	$TV = To$
	S3	$TW = Ta + To$

$$\theta_i = \theta - (k-1)\pi/3 \quad (16)$$

where  $k$  is number of sector.

$$T_a = mT_s \sin(\pi/3 - \theta_i) \quad (17)$$

$$T_b = mT_s \sin(\theta_i) \quad (18)$$

$$T_o = T_s - T_a - T_b \quad (19)$$

$T_s$  is switching period. Thus, the switching times can be obtained by using  $T_a$ ,  $T_b$  and  $T_o$  for each sector as given in Table.1.

#### IV. MODIFIED MPPT TECHNIQUE FOR MOTOR DRIVE

The MPPT should be used in solar systems to maximize the output power of the PV array not depending on the temperature, irradiation conditions and load characteristic. Generally, the MPPT is performed by dc-dc converter or battery charger. However, in this study the dc-dc converter and battery charger are not used for achieving MPPT since the PV panels are directly connected to the drive system. Therefore, the MPPT should be performed by adjusting the speed reference of the motor which is depending on the PV power.

In this case, the maximum power point of PV power should be determined for IMPP for limiting the motor current by using vector control algorithm. The characteristic of PV panel is shown in Fig.5. It can be noted that the PV power is reduced with increasing PV current. Therefore, the drive system should be operated at maximum power point PMPP and corresponding maximum current IMPP to obtain high efficiency. The maximum operation point is determined by using a modified MPPT algorithm given in Fig.6. The MPPT algorithm is performed by measuring the voltage and current of the PV array. The power of the PV array is instantly calculated by measured values. The maximum power is determined after the starting motor. PV array must supply the motor output power, power losses of motor and power losses of inverter. Therefore, the motor

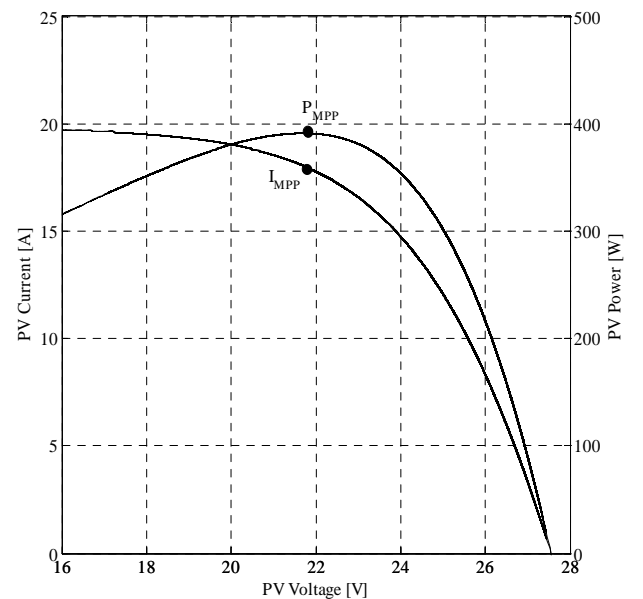


Figure 5. I-V and P-V curves to show PV characteristic with maximum point

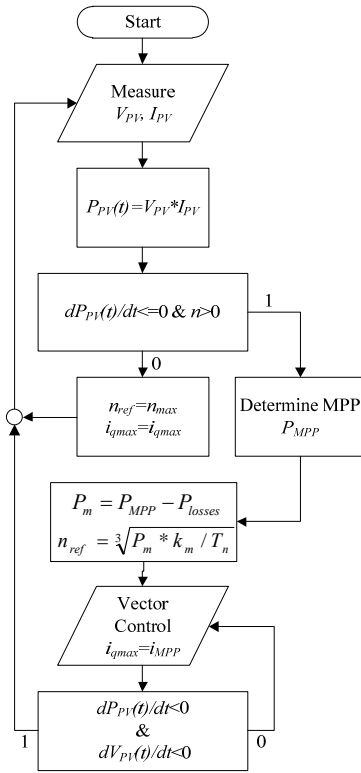


Figure 6. Modified MPPT algorithm for vector control

speed reference should be determined to operate at the maximum power point. The motor output power is calculated as given in Eq.19.

$$P_m = P_{MPP} - P_{losses} \quad (19)$$

where  $P_m$  is motor shaft power,  $P_{MPP}$  is maximum power point of the PV array and  $P_{losses}$  is total losses of the motor and inverter. The motor speed reference is calculated to obtain maximum speed since high-speed operation is generally required from the water pump motors. In this case, the motor speed reference  $n_{ref}$  is calculated as dependent on the maximum power given in Eq.20.

$$n_{ref} = \sqrt[3]{\frac{P_m \cdot k_m}{T_n}} \quad (20)$$

where  $k_m$  is the transformation constant of maximum speed,  $T_n$  is the maximum torque of the motor.  $n_{ref}$  is updated when the maximum power point is changed. Thus, the MPPT is performed by controlling the motor.

## V. THE MODELING OF THE PV ARRAY

A PV cell model can be obtained an equivalent circuit of a solar cell as shown in Fig. 7. The model consists of a current source, an anti-parallel diode connected to the source and two resistors connected in parallel and in series. The model is known as the both five-parameter model and single-diode model. The PV cell current  $I$  is calculated as Eq.21 and Eq.22.

$$I = I_{PV} - I_D - I_{Rp} \quad (21)$$

$$I = I_{PV} - I_0 \left[ \exp \left( \frac{V + R_s I}{a} \right) - 1 \right] - \frac{V + R_s I}{R_p} \quad (22)$$

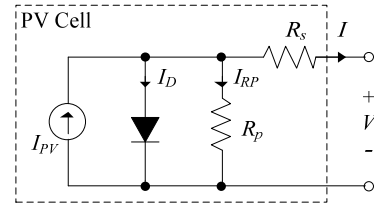


Figure 7. The equivalent circuit of a PV cell.

where  $I_0$  is the reverse saturation or leakage current of the diode. The  $a$  is modified ideality factor defined in Eq.23.

$$a = \frac{N_s n k T}{q} \quad (23)$$

where  $N_s$  is the number of cells in series,  $n$  is the diode ideality constant,  $k$  is the Boltzmann constant ( $1.3806503 \times 10^{-23}$  J/K),  $T$  is the cell temperature in Kelvin and  $q$  is the electron charge ( $1.60217646 \times 10^{-19}$  C). In addition, the characteristic of the PV cell depends on external influences such as irradiation level and temperature.

The light-generated current of the PV cell is given in Eq.24 influenced solar irradiation and temperature.

$$I_{PV} = (I_{PV,n} + K_I [T - T_n]) \frac{G}{G_n} \quad (24)$$

where  $I_{PV,n}$  is the light-generated current at  $25^\circ\text{C}$  and  $1000 \text{ W/m}^2$ ,  $T$  is actual temperature (Kelvin),  $T_n$  is the nominal temperature (Kelvin),  $G$  is the irradiation on the device surface ( $\text{W/m}^2$ ) and  $G_n$  is the nominal irradiation ( $\text{W/m}^2$ ). The simplified equation of diode saturation current  $I_0$  is defined in [20] as follows;

$$I_0 = \frac{I_{SC,n} + K_I [T - T_n]}{\exp((V_{OC,n} + K_V (T - T_n))/a) - 1} \quad (25)$$

where  $I_{SC,n}$  is the nominal short circuit current,  $V_{OC,n}$  is the nominal open-circuit voltage,  $K_I$  is the current coefficients and  $K_V$  is the voltage coefficients.

The PV model is performed by using the Eq.21 to Eq.25 in MATLAB environment as shown in Fig.8 [21].

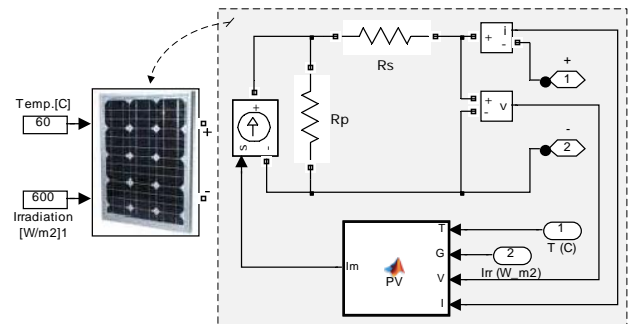


Figure 8. The MATLAB model of the PV array.

In order to demonstrate the characteristics of the PV array model is tested in different temperature and irradiation as given in Fig.9. The I-V characteristic of the PV array is shown at different temperature and same irradiation value as  $1000 \text{ W/m}^2$  in Fig.9a. The effect of the irradiation on the I-V curve is given in Fig.9b at the same temperature as  $25^\circ\text{C}$ .

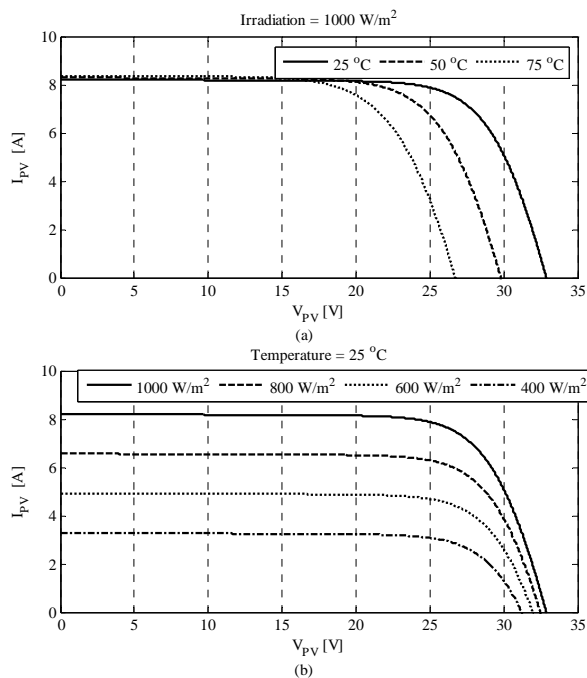


Figure 9. I-V curves; a) Different temperature conditions at 1000 W/m<sup>2</sup>, b) Different irradiation conditions at 25 °C

The validity of the results is confirmed with the [22].

## VI. REFERENCES SECTION

The simulation of solar motor drive system is performed by using MATLAB/SimPowerSystem blocks as shown in Fig.10.d in different sample time to obtain realistic results. The sample times of the control blocks model and power blocks model are taken as 100  $\mu$ s and 10 $\mu$ s, respectively.

The pump motors are generally operated to the highest possible speed as 3000 rpm. The pump motor cannot be always operated at the highest speed since the power of the

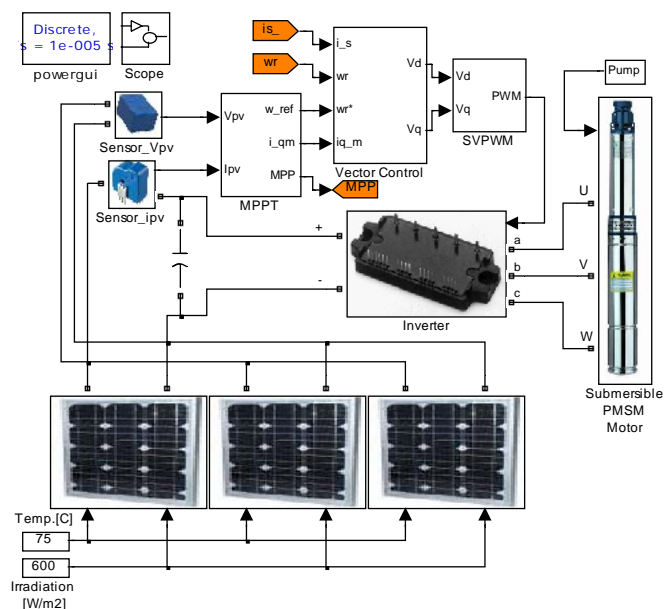


Figure 10. The system model of solar pump motor drive

PV array is affected by the irradiation and temperature. Therefore, the reference speed is simultaneously calculated using the MPPT algorithm for operating at the maximum power point.

The results of solar pump motor drive system are obtained for operating at 75 °C and 600 W/m<sup>2</sup> are given in Fig.11a to Fig.11d. The power characteristic of the PV array is shown in Fig.11a with pointed the maximum power point determined as 265W. The PV array voltage and current are changed as shown in Fig.11b. It should be noted that the PV array voltage is adjusted at the maximum power point about 20V. The three phase stator currents are given in Fig.11c. The motor speed is changed as shown in Fig.11d which is limited at the maximum available speed about 2300rpm.

As a second work, the temperature and irradiation are adjusted as 40 °C and 1000 W/m<sup>2</sup>, respectively. The results

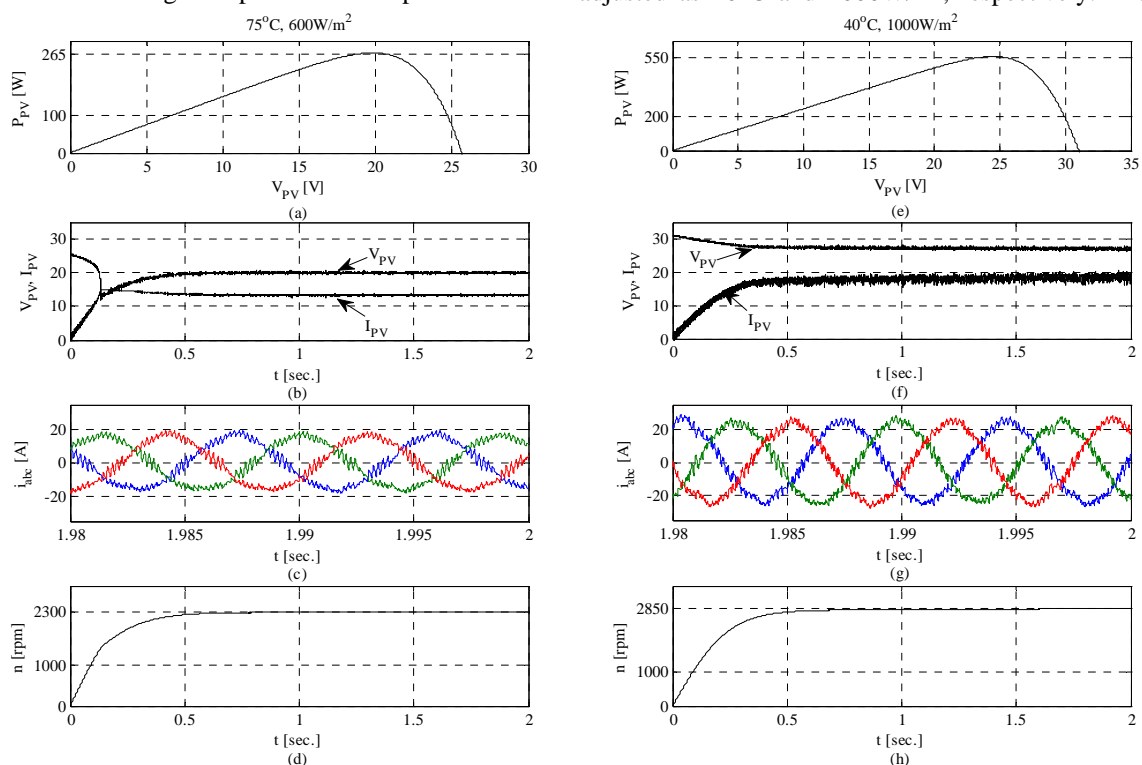


Figure 11. Operating at 75 °C and 600 W/m<sup>2</sup> conditions; a) P-V curve of PV array, b) Voltage and current of the PV array, c) Stator currents, d) Motor speed, Operating at 40 °C and 1000 W/m<sup>2</sup> conditions; e) P-V curve of PV array, f) Voltage and current of the PV array, g) Stator currents, h) Motor speed

are given in Fig.11e to Fig.11h for this adjusted condition. In this case, the maximum power point of the PV array is obtained about 550W as shown in Fig.11e. The voltage of PV array is increased from 20V to 25V as shown in Fig.11f. According to this increasing of the voltage the stator currents and motor speed are increased as shown in Fig.11g and Fig.11h. The motor speed is increased from 2300rpm to 2850rpm. The results show that the motor is operated at the maximum power point. The line voltage  $V_{ab}$  and motor current  $I_a$  are given in Fig.12a running at the steady-state operation. The harmonic spectrum of line voltage is shown in Fig.12b and the THD of  $V_{ab}$  is calculated as 43.17%. The harmonic spectrum of motor current is obtained as shown in Fig.12c. The THD of motor current is obtained in appropriate value as 5.86%.

## VII. CONCLUSIONS

A solar motor pump drive system is performed by not

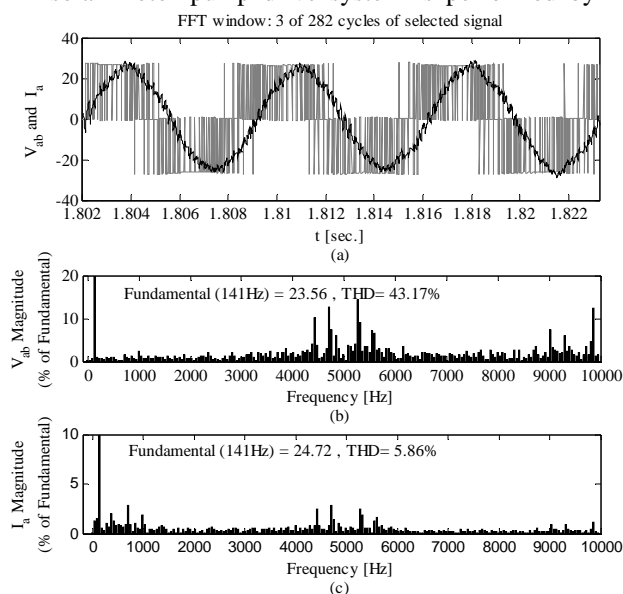


Figure 12. The results for operating at 40°C and 1000 W/m<sup>2</sup> conditions;

a) The waveforms of the line voltage  $V_{ab}$  and motor current  $I_a$ ,  
b) FFT analysis and voltage spectrum of  $V_{ab}$ , c) FFT analysis and current spectrum of  $I_a$

requiring any kind of a storage system as battery and a dc-dc converter. Thus, an efficiency and simple connection is achieved by using a direct connected PV solar system.

The simulated PV array model can be connected the MATLAB/SimPowerSystem blocks. The model is useful for developing solar system simulation that is supported with results. In this study a special motor is designed for a low rated voltage level about 24V. Thus generated voltage of the PV array is not required to increase any kind of boost converter. A vector controlled PMSM is used to increase the system efficiency and performance. The motor current is analyzed with FFT and harmonic spectrum. However, the inductance of the motor coil has low value due to the winding number is used as 10 for each coil. Therefore, the THD of motor current cannot be reduced more than 5 percent. In addition, the five-segment switching sequence is used for obtaining the SVPWM algorithm to reduce the switching losses of the inverter.

The motor speed reference is changed depending on the value of the maximum available power of the PV array. The maximum power point is continuously determined by using a modified MPPT method. The performance of motor drive

system is analyzed in different conditions as temperature and irradiation of PV array.

As a result, the direct connected PV array can be used for low voltage and low power motors to obtain simplicity and high efficiency.

## APPENDIX A

### Motor Parameters:

$V_{dc} = 20$  V;  $R_s = 0,002$   $\Omega$ ;  $L_d = 7,86 \cdot 10^{-5}$  H;  $L_q = 1,02 \cdot 10^{-4}$  H;  $p=6$ ;  
 $T_n = 1.8$  Nm;  $J = 14.68 \cdot 10^{-4}$  kg.m<sup>2</sup>;  $B = 0$  Nm s/rad.

## REFERENCES

- [1] B. K. Bose, "Global warming: Energy, environmental pollution, and the impact of power electronics," *IEEE Ind. Electron. Mag.*, vol. 4, no. 1, pp. 6–17, Mar. 2010.
- [2] Y. K. Renani, B. Vahidi and H. A. Abyaneh, "Effects of Photovoltaic and Fuel Cell Hybrid System on Distribution Network Considering the Voltage Limits," *Advances in Electrical and Computer Engineering*, vol.10, no.4, pp. 143-148, 2010.
- [3] Solar Electricity cannot serve any significant fraction of U.S. or world electricity needs [Online]. Available: <http://www1.eere.energy.gov/solar/myths.html>
- [4] BP statistical review of world energy 2009, BP Inc., 2009, p. 6, 22, 32, 40.
- [5] Nuclear energy outlook, 2008, OECD.
- [6] Survey of energy resources 2007, World Energy Council
- [7] R. Abe, H. Taoka, D. McQuilkin, "Digital Grid: Communicative Electrical Grids of the Future," *IEEE Trans. on Smart Grid*, vol. 2, no. 2, pp.399-410, 2011.
- [8] Z. Liang, R. Guo, J. Li, A.Q. Huang, "A High-Efficiency PV Module-Integrated DC/DC Converter for PV Energy Harvest in FREEDM Systems," *IEEE Trans. on Power Electronics*, vol. 26, no. 3, pp.897-909, 2011.
- [9] IMS Research. (2011, Nov. 11). [http://imsresearch.com/news-events/press-template.php?pr\\_id=2407](http://imsresearch.com/news-events/press-template.php?pr_id=2407)
- [10] G. Acciari, D. Graci, A. La Scala, "Higher PV Module Efficiency by a Novel CBS Bypass," *IEEE Trans. on Power Electronics*, vol. 26, no. 5, pp.1333-1336, 2011.
- [11] B. Yang, W. Li, Y. Zhao, X. He, "Design and Analysis of a Grid-Connected Photovoltaic Power System," *IEEE Trans. on Power Electronics*, vol. 25, no.4, pp.992-1000, 2010.
- [12] Y.H. Ji, D.Y. Jung, J.G. Kim, J.H.Kim, T.W. Lee, "A Real Maximum Power Point Tracking Method for Mismatching Compensation in PV Array Under Partially Shaded Conditions," *IEEE Trans. on Power Electronics*, vol. 26, no.4, pp.1001-1009, 2011.
- [13] Vas P. Sensorless, Vector and Direct Torque Control, Oxford Science Publications, 1998.
- [14] O.Aydogmus, "Design of Permanent Magnet Synchronous Motor Drive Fed by a Matrix Converter", PhD Thesis, *Firat University*, Elazig, Turkey, 2011.
- [15] Y. Mohammed, "Design and Implementation of a Robust Current-Control Scheme for a PMSM Vector Drive With a Simple Adaptive Disturbance Observer," *IEEE Trans. on Industrial Electronics*, vol. 54, no.4, pp.1981-1988, 2007.
- [16] T. Tudorache, M. Popescu, "Optimal Design Solutions for Permanent Magnet Synchronous Machines," *Advances in Electrical and Computer Engineering*, vol.11, no.4, pp. 77-82, 2011.
- [17] M. A. Vitorino, M. B. de R. Correa, C. B. Jacobina, A. M. N.Lima, "An Effective Induction Motor Control for Photovoltaic Pumping," *IEEE Trans. on Industrial Electronics*, vol. 58, no.4, pp.1162-1170, 2011.
- [18] O.Wallmark, "Control of a Permanent Magnet Synchronous Motor with Non-Sinusoidal Flux Density Distribution", MSc Thesis, *Chalmers University of Technology*, Göteborg, Sweden, 2001.
- [19] S.Sünter and H.Altun, "Control of A Permanent Magnet Synchronous Motor Fed By A Direct AC-AC Converter", *Electrical Engineering*, vol. 87, no. 2, pp. 83-92, 2005.
- [20] B. Wu, "High-Power Converters and AC Drives," *New Jersey: Wiley-Interscience*, 2006.
- [21] Math Works Inc., *MATLAB*, Licence ID: 585775.
- [22] M. G. Villalva, J. R. Gazoli, and E. R.Filho, "Comprehensive Approach to Modeling and Simulation of Photovoltaic Arrays," *IEEE Trans. on Power Electronics*, vol. 24, no.5, pp.1198-1208, 2009.